IEEE Access
Multidisciplinary ⋮ Rapid Review ⋮ Open Access Journal

Received December 21, 2020, accepted January 2, 2021, date of publication January 5, 2021, date of current version January 20, 2021.

Digital Object Identifier 10.1109/ACCESS.2021.3049395

The Ossanna's Theorem for Educational Purposes: Impact of Distributed Parameter Transmission Lines on Power Systems

ROBERTO BENATO, (Senior Member, IEEE), AND SEBASTIAN DAMBONE SESSA, (Member, IEEE)
Department of Industrial Engineering, University of Padova, 35131 Padova, Italy
Corresponding author: Roberto Benato (roberto.benato@unipd.it)

ABSTRACT This paper faces a challenge in power education: how to teach the students the impact of different transmission lines on the power system at power frequency. More specifically, the paper exploits the very effective and elegant Ossanna's theorem in order to make clear which are the allowable electrical regimes of different transmission line typologies in terms of power losses, voltage drops, transmissible powers and the conditions for the voltage collapse. Moreover, the formulation of the complex power at the sending-end of the power transmission line inferred from the Ossanna's theorem, which has never been shown in technical literature, is clearly presented. It is worth noting that although the paper is focused on high and extra-high voltage transmission lines, the presented didactical approach can be indifferently applied to any voltage level.

INDEX TERMS Ossanna's theorem, power education, power losses, transmission lines, voltage drops.

I. INTRODUCTION

This paper presents the experiences of the Department of Industrial Engineering at the University of Padova in the extensive use of Ossanna's theorem [1], [2] for educational purpose, together with other original formulae never presented in scientific literature.

Ossanna is well known in scientific literature for his circle diagram. However, he was also involved in the analysis of very long (up to 1000 km) high voltage (220 kV) shunt compensated overhead lines, where he developed the very effective theorem applied in this paper. Maybe the German language (his work was also translated in Italian language in a paper of the Journal named L'Elettrotecnica in 1923) or the presence of his famous circle diagram meant that the theorem recovered in this paper fell on deaf ears: on the contrary, the authors are convinced that it ought to be also appreciated as one of the more important tool in the circuit theory.

In particular, the methodology described in the paper makes the students able to clearly understand the concept of allowable steady state regimes of different transmission lines, which is not straightforward, but which is very important in the electrical engineer formation. The students at the end of a power systems course should be able to answer easily the following questions: which is the transmissible power of an electric line? Which are the power losses and the voltage drops? Is a given steady-state regime allowable and physically feasible inside the grid?

These questions encompass the student brains and power education needs to give the students an effective tool to answer them. Several books [3]–[8] face these issues since they generally deal with the electrical lines modelled by a single-phase circuit with distributed parameters. There is no doubt that a more traditional approach based only on power flow analyses by including a transmission line typology rather than another, is also possible. However, the use of power flow tools alone does not allow the students to focus on the transmission line performances. Furthermore, if the power flows are performed only by means of commercial software, the student minds are captured by how the software works rather than how a transmission line electrically behaves. Therefore, an analytical and self-implementable algorithm has been felt as necessary: at the University of Padova, this has been achieved by the Ossanna's method together with some other original formulae deriving from the known transmission equations, which are completely expounded in this paper.

The associate editor coordinating the review of this manuscript and approving it for publication was Hui Ma.

By implementing the described procedures in any mathematical software (Matlab is used in the advanced power systems course at Padova University, but others are possible) the students have a powerful ally to effectively understand both the role and the behaviour of different transmission lines in the power system.

II. NOMENCLATURE

pul:	per unit length and *pu* per unit;
d:	line length;
S and R:	subscripts for sending-end and receiving-end;
r:	pul longitudinal resistance [Ω/km];
ℓ:	pul longitudinal inductance [mH/km];
g:	pul shunt conductance [S/km];
c:	pul shunt capacitance [F/km];
$\underline{z} = r + \mathrm{j}\omega\ell$:	pul longitudinal impedance [Ω/km];
$\underline{y} = g + \mathrm{j}\omega c$:	pul shunt admittance [S/km];
$\underline{A}$, $\underline{B}$, $\underline{C}$, $\underline{D}$:	elements of the transmission matrix $\underline{\mathbf{M}}$;
$\underline{k} = k' + \mathrm{j}k''$:	propagation constant [1/km];
$\underline{Z}_c$:	characteristic impedance [Ω];
$\underline{\boldsymbol{w}}_{\boldsymbol{S}}$, $\underline{\boldsymbol{w}}_{\boldsymbol{R}}$:	voltage and current vectors at sending-end and at receiving-end;
$\underline{S}_{nat}$:	characteristic or natural power;
$\underline{S}_R$:	three-phase complex power fixed at receiving-end;
$\underline{S}_{oR} = S_{oR}\, e^{j\varphi}$:	single-phase power fixed at receiving-end;
$\underline{I}_{Rsc}$:	short circuit current at R;
$\underline{U}_{oRNL}$:	voltage of the Thevenin equivalent generator;
$\underline{Z} = Ze^{j\psi}$:	impedance of the Thevenin equivalent generator;
$\underline{u} = ue^{j\delta}$:	pu unknown voltage at receiving-end with the real and imaginary components u_x and u_y;
U_{ob}, Z_b, S_{ob}:	basis voltage, impedance and power for pu method;
α:	argument of $\underline{A}$;
I''_{sc}:	three-phase subtransient short circuit magnitude;
Δu, Δp, ΔP, ΔQ:	percent voltage drop, percent Joule losses, Joule losses [MW], reactive power required by the line [Mvar];
$\underline{I}_{NL}$:	current at no-load;
$\underline{U}''_{oR}$:	no-load power frequency sub-transient voltage;
$\underline{u}_1$, $\underline{u}_2$:	two possible solutions of the Ossanna's theorem.

III. ELECTRIC LINES MODELLED WITH DISTRIBUTED PARAMETERS: BRIEF RECALLS

The geometrical structure of an overhead line always implies an asymmetric system, which cannot be licitly studied by means of a positive sequence equivalent circuit. The possibility of line symmetrisation, e.g. by means of phase transpositions, is not always feasible. Anyway, it is well known that the approximations introduced by the hypothesis of perfect structural symmetry are wholly acceptable as a first orientation. For other transmission line typologies, the situation is much closer to a symmetric structure. In fact, for cable lines, the asymmetry is limited since the external electric field is zeroed by screen bonding and earthing. For Gas Insulated Lines, the zeroing of external electric and magnetic fields implies a perfect electric and magnetic decoupling between the three phases so that the system is completely symmetric and licitly representable by means of an equivalent single-phase positive sequence circuit.

Hence, in the hypothesis of a symmetric transmission line, it is possible to refer to a positive sequence equivalent circuit.

The knowledge of the pul distributed parameters r, ℓ, c and g representing the transmission line, as a positive sequence equivalent circuit, allows computing the propagation constant $\underline{k}$ and the characteristic impedance $\underline{Z}_c$ [3]–[8] as follows:

$$\underline{k} = \sqrt{\underline{z} \cdot \underline{y}} \quad [1/\mathrm{km}] \text{ and } \underline{Z}_c = \sqrt{\underline{z} \Big/ \underline{y}}\ [\Omega].$$

Let us introduce the two transmission equations (1) and (2), which are commonly used to express the voltage ((1)) and current ((2)) at the sending-end of a transmission line as a function of the receiving-end current and voltage:

$$\underline{U}_{oS} = \underline{A} \cdot \underline{U}_{oR} + \underline{B} \cdot \underline{I}_R \tag{1}$$

$$\underline{I}_S = \underline{C} \cdot \underline{U}_{oR} + \underline{D} \cdot \underline{I}_R; \tag{2}$$

with: $\underline{A} = cosh\left(\underline{k}d\right)$; $\underline{B} = \underline{Z}_c \cdot sinh\left(\underline{k}d\right)$; $\underline{C} = \left[sinh\left(\underline{k}d\right)\right]/\underline{Z}_c$; $\underline{D} = cosh\left(\underline{k}d\right)$. The eqs. (1) and (2) can be rearranged in the concise elegant matrix form, where $\underline{\boldsymbol{M}}$ is often named transmission matrix [3]–[8],

$$\underbrace{\begin{bmatrix} \underline{U}_{oS} \\ \underline{I}_S \end{bmatrix}}_{\underline{\boldsymbol{w}}_{\boldsymbol{S}}} = \underbrace{\begin{bmatrix} \underline{A} & \underline{B} \\ \underline{C} & \underline{D} \end{bmatrix}}_{\underline{\mathbf{M}}} \cdot \underbrace{\begin{bmatrix} \underline{U}_{oR} \\ \underline{I}_R \end{bmatrix}}_{\underline{\boldsymbol{w}}_{\boldsymbol{R}}} \tag{3}$$

which allows obtaining the vector $\underline{\boldsymbol{w}}_{\boldsymbol{S}}$ at sending-end once fixed the vector $\underline{\boldsymbol{w}}_{\boldsymbol{R}}$ at receiving-end. In order to express the vector $\underline{\boldsymbol{w}}_{\boldsymbol{R}}$ at receiving-end, as a function of the vector $\underline{\boldsymbol{w}}_{\boldsymbol{S}}$ at sending-end, the matrix formulation changes as follows:

$$\underbrace{\begin{bmatrix} \underline{U}_{oR} \\ \underline{I}_R \end{bmatrix}}_{\underline{\boldsymbol{w}}_{\boldsymbol{R}}} = \underbrace{\begin{bmatrix} \underline{D} & -\underline{B} \\ -\underline{C} & \underline{A} \end{bmatrix}}_{\underline{\boldsymbol{M}}_{\boldsymbol{a}}} \cdot \underbrace{\begin{bmatrix} \underline{U}_{oS} \\ \underline{I}_S \end{bmatrix}}_{\underline{\boldsymbol{w}}_{\boldsymbol{S}}}; \quad \underline{\boldsymbol{M}}_{\boldsymbol{a}} = \underline{\boldsymbol{M}}^{-\mathbf{1}}. \tag{4}$$

It is easy to demonstrate that $\underline{\boldsymbol{M}}_{\boldsymbol{a}}$ is the inverse of $\underline{\boldsymbol{M}}$, by remembering that, $\underline{A}\ \underline{D} - \underline{B}\ \underline{C} = 1$ in virtue of the reciprocity principle [3]–[8].

IV. THE OSSANNA'S THEOREM APPLIED TO THE EQUIVALENT POSITIVE-SEQUENCE CIRCUIT OF ANY TRANSMISSION LINE

Ossanna's theorem [1], [2] analytically solves the regimes of any electric line modelled by its equivalent single-phase circuit when a voltage phasor is applied at its sending-end and a three-phase complex power $\underline{S}_R$ is fixed at its receiving-end.

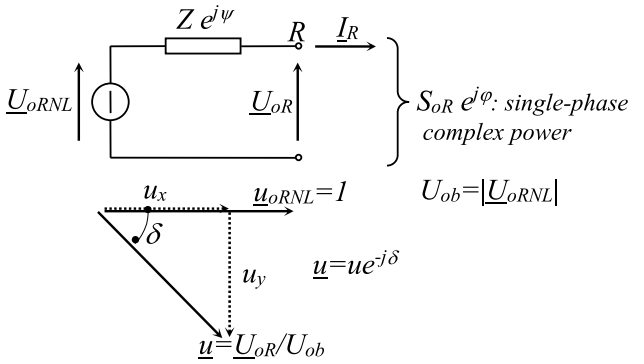

FIGURE 1. Single-phase model as seen at port R and phasor $\underline{u}$ (pu).

It constitutes a powerful tool to investigate the steady state regimes and can determine the limit conditions of physical feasibility of the line operation. Of course, in the hypothesis of constraining the voltage phasor at receiving-end, there would be no need to refer to Ossanna's theorem, but such assumption is theoretically mistaken and inelegant.

In fact, by knowing the three-phase complex power at receiving-end of a line, the current would be immediately known and consequently the voltage and current at sending-end would be known as well. This is because the sending-end voltage and current are linked to the receiving-end ones by means of (3).

A more traditional approach involves an iterative procedure instead of the Ossanna's theorem to solve the electrical regime of transmission lines. In summary, in such procedure a voltage phasor magnitude is tentatively hypothesized at receiving-end; then, the current absorbed by the load is easily computed (by knowing the complex power fixed at receiving-end) and by means of the transmission equations (1) and (2), the voltage magnitude (and current) at the sending-end is computed and compared with the fixed one.

The iterations stop when the magnitude of computed sending-end voltage differs from the fixed one by a given mismatch (see Appendix).

However, this method is cumbersome since the number of necessary iterations increases significantly by increasing the chosen precision (see Appendix). In this context, one of the major points of strength of the Ossanna's theorem is that it allows using a direct analytical solution and avoiding iterative procedures.

Given the single-phase modelling of a three-phase network seen at the R port, the Ossanna's method determines, at the port itself, the possible voltage regimes (and consequently the current ones) due to a fixed absorbed complex power (for each phase) $\underline{S}_{oR} = S_{oR}\, e^{j\varphi} = \underline{S}_R/3$.

It is very useful, in this analysis, to represent the line by means of its equivalent Thevenin generator as seen at the port R, as it is shown in Fig. 1. The values of Thevenin equivalent voltage source and impedance can be derived from (1) and (2) as in (5) and (6):

$$\underline{U}_{oRNL} = \frac{U_{oS}}{\underline{A}} \tag{5}$$

$$\underline{Z} = \frac{\underline{U}_{oRNL}}{\underline{I}_{Rsc}} = \frac{U_{oS}/\underline{A}}{U_{oS}/\underline{B}} = \frac{\underline{B}}{\underline{A}} = Z\ e^{j\psi} \tag{6}$$

being $\underline{I}_{Rsc}$ = short circuit current at the R port.

Hence, by applying the second Kirchhoff's law, (7) can be written as:

$$\frac{\underline{U}_{oRNL} - \underline{U}_{oR}}{\underline{Z}} = \underline{I}_R = \left(\frac{\underline{S}_{oR}}{\underline{U}_{oR}}\right)^{*}. \tag{7}$$

If the pu method is adopted and by assuming the following basis quantities

$$U_{ob} = |\underline{U}_{oRNL}|\ S_{ob} = \frac{U_{ob}^2}{|\underline{Z}|} \quad Z_b = |\underline{Z}|$$

and by posing $\underline{U}_{oRNL}$ on the real axis, the following pu relations can be obtained:

$$\frac{1-\underline{u}}{e^{j\psi}} = \underline{i} = \frac{\underline{s}^*}{\underline{u}^*} \Rightarrow \underline{u}^* - u^2 = \underline{s}^*\, e^{j\psi} \Rightarrow u\, e^{j\delta} - u^2 = s\, e^{j(\psi-\varphi)} \Rightarrow u^2 - u\, e^{j\delta} + s\, e^{j\chi} = 0 \tag{8}$$

where $\frac{\underline{U}_{oRNL}}{U_{ob}} = u_{oRNL} = 1$; $\underline{u} = \frac{\underline{U}_{oR}}{U_{ob}}$; $u = |\underline{u}|$; $\underline{u} = u\, e^{-j\delta}$; $\frac{\underline{Z}}{Z_b} = e^{j\psi}$; $\underline{s} = \frac{\underline{S}_{oR}}{S_{ob}}$; $\underline{s} = s e^{j\varphi}$; $\psi - \varphi = \chi$.

By explicating the real and the imaginary parts of the unknown voltage in (8), the following system of equations is obtained

$$\begin{cases} u_x^2 + u_y^2 - u_x + s\ \cos\chi = 0 & (9) \\ -u_y + s\ \sin\ \chi = 0 & (10) \end{cases}$$

so that the u_y component is derived from (10), i.e.

$$u_y = s \cdot sin\chi \tag{11}$$

and it allows transforming (9) in (12):

$$u_x^2 + (s \cdot sin\chi)^2 - u_x + s \cdot cos\chi = 0 \Rightarrow u_x^2 - u_x + [s \cdot cos\chi + (s \cdot sin\chi)^2] = 0. \tag{12}$$

From (12), two analytical solutions yield:

$$u_x = \frac{1 \pm \sqrt{1 - 4\left[s\,cos\chi + (s\,sin\chi)^2\right]}}{2} = \frac{1}{2} \pm \sqrt{\frac{1}{4} - s\,cos\chi - (s\,sin\chi)^2}$$

$$u_x = 1/2 \pm \zeta_{Oss}; \tag{13}$$

$$\text{where } \zeta_{Oss} = \sqrt{\frac{1}{4} - s\,cos\chi - (s\,sin\chi)^2} \tag{14}$$

Since ζ_{Oss} must be real, this constrain gives the condition of physical feasibility.

Therefore, it is possible to determine *analytically* the two pu phasors $\underline{u}_1$ and $\underline{u}_2$ at the port R, each of them compatible with the same pu fixed power $\underline{s}$:

$$\underline{u}_1 = [(1/2) + \zeta_{Oss}] - j[u_y] \tag{15}$$

$$\underline{u}_2 = [(1/2) - \zeta_{Oss}] - j[u_y] \tag{16}$$

$$\zeta_{Oss} \geq 0 \tag{17}$$

being (17) the constraint of physical feasibility.

It can be ascertained that the phasor $\underline{u}_2$, in (16), always presents very small magnitudes (with consequently higher currents) and it can be exploited as a precise reference for possible investigations of the voltage collapse conditions. Hence, if the objective of the transmission line study is to investigate the allowable regimes, only (15) must be taken into account. From (15) and (16), it is immediate to derive the relation $\underline{u}_1 + (\underline{u}_2)^* = 1 = \underline{u}_2 + (\underline{u}_1)^*$, which clearly highlights how, if $\underline{u}_1$ is close to 1, the same cannot be for $\underline{u}_2$.

A. THE DERIVATION OF A DIRECT FORMULA FOR ESTIMATING THE COMPLEX POWER AT SENDING-END

In order to compute the power losses $\Delta p = 3 \cdot \text{real}(\underline{S}_{oS} - \underline{S}_{oR})$ and the whole reactive power required by the line $\Delta q = 3 \cdot \text{imag}(\underline{S}_{oS} - \underline{S}_{oR})$, it is necessary to compute the complex power at sending-end $\underline{S}_S$. In order to obtain such fundamental formula (*not shown in the Ossanna's papers and never published in technical literature*), the equivalent generator scheme as seen at sending-end must be considered.

From (4), it is immediate to write the current $\underline{I}_S$ as:

$$\underline{I}_S = \frac{\underline{S}^*_{oS}}{\underline{U}^*_{oS}} = \frac{\underline{D}\,\underline{U}_{oS} - \underline{U}_{oR}}{\underline{B}}$$

and by means of some simple passages; it is

$$\frac{\frac{\underline{D}\,\underline{U}_{oS}}{\underline{A}} - \underline{U}_{oR}/\underline{A}}{\underline{B}/\underline{A}} = \frac{\frac{\underline{D}\,\underline{A}\,\underline{U}_{oRNL}}{\underline{A}} - \underline{U}_{oR}/\underline{A}}{\underline{B}/\underline{A}} = \frac{\underline{D}\,\underline{U}_{oRNL} - \underline{U}_{oR}/\underline{A}}{\underline{Z}} = \frac{\underline{S}^*_{oS}}{\underline{U}^*_{oS}}$$

If, once again, the same basis quantities of Sect IV are adopted, the complex power at the sending-end is obtained as in (18):

$$\underline{i}_S = \frac{\underline{s}^*_S}{\underline{A}^*} = \frac{\underline{D} - \underline{u}_{oR}/\underline{A}}{e^{j\psi}} \rightarrow \underline{s}_S = \left(\underline{A}\,\underline{D}^* - \underline{u}^*_{oR} e^{j2\alpha}\right) e^{j\psi} \quad (18)$$

where α is the argument of $\underline{A}$ and $\underline{u}_{oR}$ is given by (15).

Eq. (18) is completely general and it has never been published before. In case of symmetric line with $\underline{D} = \underline{A}$, (18) becomes the simpler one [9]:

$$\underline{s}_S = \left(A^2 - \underline{u}^*_{oR} e^{j2\alpha}\right) e^{j\psi}.$$

B. THE NO-LOAD ENERGIZATION OF ELECTRIC LINES INSIDE THE GRID AND ITS DE-ENERGIZATION

In order to understand the behaviour of a given transmission line, the electrical engineering students should be able to easily answer the following questions: what happens when a no-load electric line is energized and de-energized? How does a weak (i.e. low fault levels) or strong (i.e. high fault levels) grid condition overvoltages and no-load currents?

Let us consider the simplified sketch of Fig. 3, which shows the switch-on of a circuit breaker in the point S of a given line in order to energize it. It serves as a first *didactical approach* devoted to highlight the limit conditions for line energisation at no-load.

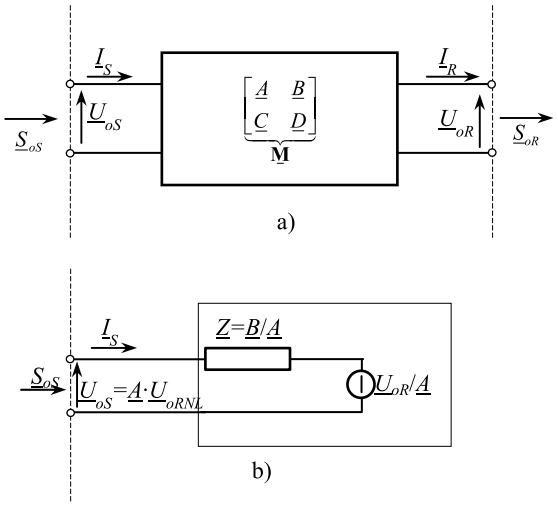

FIGURE 2. a) Indication of complex powers at sending and receiving ends; b) Equivalent generator as seen at sending-end.

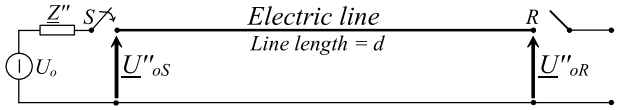

FIGURE 3. No- load energization at port S.

In a generic network, the power supply in S can be modelled as an equivalent generator characterized by an electromotive force U_o (supposed to be equal to the nominal phase-to-earth voltage) and a short-circuit subtransient impedance $\underline{Z}''$ (for simplicity assumed as purely inductive, i.e. $\underline{Z}'' = jX$). The magnitude of the sub-transient voltage $\underline{U}''_{oR}$ at the power frequency and no-load condition at the port R, following the closure of the circuit breaker is completely defined through the following formulae:

$$\underline{U}''_{oS} = \left(\frac{U_o}{\underline{Z}'' \cdot + \frac{\underline{A}}{\underline{C}}}\right) \cdot \frac{\underline{A}}{\underline{C}} \quad (19)$$

$$\underline{U}''_{oR} = \frac{\underline{U}''_{oS}}{\underline{A}} \quad (20)$$

$$\underline{U}''_{oR} = \frac{U_o}{\underline{A} + \underline{Z}'' \cdot \underline{C}} \quad (21)$$

It is worth reminding that (20) expresses the Ferranti's effect.

With regard to the evaluation of $\underline{Z}''$, it is possible to refer to the relationship $\underline{Z}'' = U_o/I''_{sc}$. For example, in case of considering a 400 kV grid, the values of the subtransient short circuit current I''_{sc} (three-phase short circuit at S) can be foreseen in the range of *10-50* kA, whereas the values of the reactance X ranges between *23-4,6* Ω. In order to respect the standard switching levels (e.g. 1050 kV for $U_r = 400$ kV) with a conservative margin, it seems advisable that the phasor $\underline{U}''_{oR}$ does not exceed the magnitude $U_m/\sqrt{3}$ (e.g. = 242,5 kV for $U_r = 400$ kV and $U_m = 420$ kV).

In the hypothesis that, once the transient phenomena are extinguished, the voltage regulation system of the grid restores again the rated value $U_o = 230$ kV at port S, it is

TABLE 1. Preferred values of rated capacitive switching currents adapted from [10].

	Overhead line	*Cable line*
Rated voltage U_r [kV *r.m.s.*]	*Rated line-charging breaking current* I_ℓ [A *r.m.s*]	*Rated cable charging breaking current* I_c [A *r.m.s.*]
3,6	**10**	**10**
12	**10**	**25**
24	**10**	**31,5**
36	**10**	**50**
52	**10**	**80**
72,5	**10**	**125**
145	**50**	**160**
245	**125**	**250**
420	**400**	**400**
550	**500**	**500**
800	**900**	/

possible to compute the no-load steady state current $\underline{I}_{NL}$:

$$\underline{I}_{NL} = \frac{U_o}{\left(\underline{A}/\underline{C}\right)} \tag{22}$$

$\underline{I}_{NL}$ is the current which the circuit breaker b must be able to interrupt in case of de-energization of the no-load line. For this current the Standards on the Circuit Breaker (§4.107 of [10]) suggest the limit values of Table 1.

Eventually, the students must check that both the following additional constraints are fulfilled

$$\left|\underline{U}''_{oR}\right| \leq U_m/\sqrt{3} \tag{23}$$

$$|\underline{I}_{NL}| \leq I_\ell \quad \text{or} \quad |\underline{I}_{NL}| \leq I_c \tag{24}$$

V. APPLICATIONS

Given that each professor can apply the approach presented in Sect. IV to the line typologies and voltage levels that he considers to be of much efficacy in relation to his course, in the following some possible applications to extra high voltage transmission lines are presented. More specifically, an overhead line, an insulated cable line and a gas-insulated line. The characteristics of these lines are shown in Table 2. In Table 2, beyond the pul parameters necessary for the computation of $\underline{k}$ and $\underline{Z}_c$, also the current rating I_{cur_rat} (often called ampacity) is reported, so that it is possible to compute the receiving-end complex power at I_{cur_rat}, i.e.

$$\underline{S}_R = \sqrt{3} U_R I_{cur\_rat} \cdot (\cos\varphi + j \sin\varphi) \tag{25}$$

The power factor cosφ can be set freely: in extra high voltage, a typical setting is cos$\varphi = 0{,}98$.

A. OVERHEAD LINES [11]–[13] WITH LENGTHS OF 300 AND 50 km

The natural power $\underline{S}_{nat}$ [3]–[8] with reference to the voltage $U_r = 400$ kV (see Table 2) is given by:

$$\underline{S}_{nat} = \frac{U_r^2}{\underline{Z}_c^*} = \frac{400000^2}{255{,}97 + \text{j}9{,}5394} = 624{,}21\text{-j}23{,}263 \ \left[\text{MW} + \text{jMvar}\right]$$

whose magnitude is $|\underline{S}_{nat}| = 624{,}64$ [MVA]. From the power transmission theory, it is well known that for a real line operated at the natural power the percent voltage drop Δu, the percent power losses Δp and the percent reactive power required by the line Δq are given by:

$$\begin{cases} \Delta u \cong k'd = 1{,}28\% \\ \Delta p \cong 2 \cdot k'd = 2{,}56\% \\ \Delta q \cong 2 \cdot k'd = 2{,}56\% \end{cases} \tag{26}$$

where k' is the attenuation constant (real part of the propagation constant in Table 2). The complex power at current rating I_{cur_rat}, is given by (25) i.e.

$$\underline{S}_R = \sqrt{3} \cdot 400000 \cdot 2955 \cdot (0{,}98 + j0{,}2) \cong 2006 + j407 \ [MW + jM\text{var}]$$

By means of (15), the students can realize how $\zeta_{Oss} < 0$ so that this complex power is not physically feasible for $d = 300$ km. Moreover, Table 3 reports several regimes that the electrical engineering students should be able to solve: such regimes are all very close to $\underline{S}_{nat}$ (two are equal to it). The conclusion is that an overhead line of such length cannot transmit a power that is much higher than the natural one: the row 3 of Table 3 shows that even $\underline{S}_R = 700 + \text{j}140$ [MW + jMvar] gives unacceptable voltage drops (about 20%!).

The second row of Table 3 allows the students to verify that if the line is operated at natural power with fixed voltage $U_{oS} = 233{,}94$ kV (so to have the same phase-to-earth voltage at receiving-end used to compute $\underline{S}_{nat}$ i.e. $400/\sqrt{3} = 230{,}97$ kV), the Δu and both $\Delta p/\Delta q$ are practically equal to those theoretically foreseen in (26). If the length of the line were 50 km as in Table 4, a student could realize how the OHL can transmit power much higher than $\underline{S}_{nat}$ up to that related to the current rating. The electrical engineering students can build a lot of tables for different line lengths, like Table 3 and 4, so to realize the following conclusions:

- if the OHL is relatively short (about d $\leq$ 150 km), it can transmit power much higher than $\underline{S}_{nat}$ (up to about three times);
- if the OHL is relatively long i.e. d $>$ 150 km, the transmissible power must be very close to $\underline{S}_{nat}$.

Regarding the aspects deriving from the line energization, I''_{sc} ranges between 10,8 kA (lowest fault level) and 50,8 kA (highest fault level) in the Italian extra high voltage grid. This implies the two equivalent reactance limits X_{weak} and X_{strong}:

$$X_{weak} = \frac{U_0}{I''_{sc}} = \frac{230000}{10500} = 21{,}905 \ [\Omega];$$

$$\underline{Z}''_{weak} \cong jX_{weak} = j21{,}905$$

$$X_{strong} = \frac{U_0}{I''_{sc}} = \frac{230000}{50800} = 4{,}5276 \ [\Omega];$$

$$\underline{Z}''_{strong} \cong jX_{strong} = j4{,}5276$$

TABLE 2. Application of the present education approach to the extra high voltage transmission lines.

OVERHEAD LINE U_r=400 kV	INSULATED CABLE U_r=400 kV	GAS-INSULATED LINE U_r=400 kV
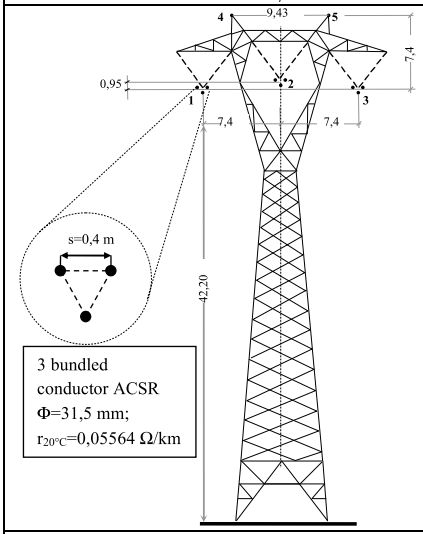	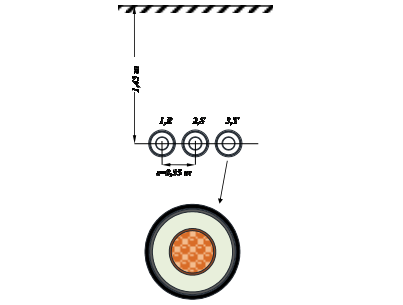 Cross-section·and·material: mm² — 2500/Cu·Milliken Conductor: mm — 63,4 Semiconductive·layer: mm — 69,5 Insulating·material·XLPE: mm — 119,9 Semiconductive·layer: mm — 127,7 Metallic·screen: mm — 130,1/Allumimum External·jacket·PE: mm — 141,7 $r_{dc,20°C}$: mΩ/km — 7,2 tanδ@50·Hz: — 0,0007 ε_r: — 2,3	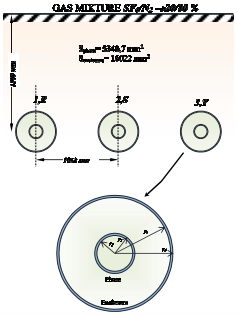 Inner·conductor·radius·r_1: mm — 80 Outer·conductor·radius·r_2: mm — 90 Inner·enclosure·radius·r_3: mm — 250 Outer·enclosure·radius·r_4: mm — 260 **Phase·conductor** Material: — Al·alloy,·EN·AW·6101B E-Al/MgSi0,5·T6·W19 Resistivity·@·20°C: Ω·mm²/m — 0,02826 **Enclosure** Material: — Al·alloy,·EN·AW·5754 AL·Mg3·W19 Resistivity·@·20°C: Ω·mm²/m — 0,03280
d=300 km and d=50 km	d=30 km	d=100 km
$r_{50°C}$=21 mΩ/km	$r_{90°C}$=12,5 mΩ/km	r=8,616 mΩ/km
ℓ=0,8591 mH/km	ℓ=0,576 mH/km	ℓ=0,2144 mH/km
c=13 nS/km	c=234 nF/km	c=54,5 nF/km
g=13,13 nS/km	g=51,459 nS/km	g=0 nS/km
$\underline{k}$=42,687·10^{-6}+j1,056·10^{-3} 1/km	$\underline{k}$=0,12718·10^{-3}+j3,6494·10^{-3} 1/km	$\underline{k}$=68,545·10^{-6}+j1,0761 10^{-3}1/km
$\underline{Z}_C$=255,97-j 9,5394 Ω	$\underline{Z}_C$=49,644-j1,695 Ω	$\underline{Z}_C$=62,849-j4 Ω
$\underline{I}_{cur\_rat}$=2955 A	$\underline{I}_{cur\_rat}$ =1788 A	$\underline{I}_{cur\_rat}$ =2390 A

TABLE 3. Steady-state regimes of the overhead line of table 2 with d = 300 km.

$\underline{S}_R$ [MW+jMvar]	$\frac{\underline{Q}_R}{P_R}$	$\lvert\underline{U}_{oR}\rvert$ kV	$\lvert\underline{U}_{oS}\rvert$ kV	ϑ °	Δu %	ΔP MW	ΔQ Mvar	Δ_p %	$\lvert\underline{I}_R\rvert$ A	$\lvert\underline{I}_S\rvert$ A	$\frac{\max(I_R,I_S)}{I_{cur\_rat}}$
624-j23,3	0,04	225,98	230	18,64	1,78	16,81	15,44	2,69	921,4	929,1	0,314
624-j23,3	0,04	230,97	233,94	17,91	1,286	16,19	-0,713	2,59	901,5	913,1	0,309
700+j140	0,2	191,6	230	24,5	20,04	28,03	190,46	4	1241,9	1158,7	0,42
750+j150	0,2	181,22	230	28,02	26,91	35,87	300,7	4,78	1406,8	1313	0,476
800+j160	0,2	160,48	230	34,45	43,29	51,98	525,31	6,5	1694,3	1584,6	0,573
800+j160	0,2	198,16	242,5	25,76	22,37	34,18	254,36	4,27	1372,3	1280,4	0,464

TABLE 4. Steady-state regimes of the overhead line of table 2 with d = 50 km.

$\underline{S}_R$ [MW+jMvar]	$\frac{\underline{Q}_R}{P_R}$	$\lvert\underline{U}_{oR}\rvert$ kV	$\lvert\underline{U}_{oS}\rvert$ kV	ϑ °	Δu %	ΔP MW	ΔQ Mvar	Δ_p %	$\lvert\underline{I}_R\rvert$ A	$\lvert\underline{I}_S\rvert$ A	$\frac{\max(I_R,I_S)}{I_{cur\_rat}}$
1000+j200	0,2	223,879	230	4,931	2,734	7,316	60,879	0,732	1518,4	1508	0,514
1200+j240	0,2	222,321	230	5,962	3,454	10,646	103,923	0,887	1834,8	1824	0,621
1400+j280	0,2	220,658	230	7,013	4,233	14,680	156,039	1,049	2156,8	2145,4	0,730
1600+j320	0,2	218,884	230	8,087	5,078	19,464	217,794	1,216	2484,8	2473,1	0,841
1800+j360	0,2	216,987	230	9,186	5,997	25,047	289,860	1,392	2819,9	2807,7	0,954
2000+j400	0,2	214,957	230	10,314	6,998	31,494	373,038	1,575	3162,8	3150,2	1,070

Eq. (21) gives the two overvoltage limits for the weakest node and for the strongest one i.e.:

$$\underline{U}''_{oR} = \frac{U_0}{\underline{A} + Z''_{strong} \cdot \underline{C}} = 243430\text{-}j1030,4\ V \rightarrow \left|\underline{U}''_{oR}\right| \cong 243,4\,kV$$

$$\underline{U}''_{oR} = \frac{U_0}{\underline{A} + Z''_{weak} \cdot \underline{C}} = 249010\text{-}j1088,4\ V \rightarrow \left|\underline{U}''_{oR}\right| \cong 249\,kV$$

Eq. (23) must be particularized for the chosen voltage level $U_r = 400$ kV: IEC standard gives $U_m = 420$ kV so that:

$$\left|\underline{U}''_{oR}\right| \leq 420/\sqrt{3} = 242,5\ \text{kV}$$

In both cases, the overvoltages exceed the constraint. Regarding the no-load switching current, it is:

$$\underline{I}_{NL} = \frac{U_0}{\underline{A}/\underline{C}} = 1,7638 + j294,58 = 294,59e^{j89,66°}\ [A]$$

In order to verify (24), Table 1 gives the value of 400 A so that:

$$|\underline{I}_{NL}| \leq I_\ell = 400\ A$$

which is verified.

B. INSULATED CABLES [14]–[19]

The natural power $\underline{S}_{nat}$ with reference to the voltage $U_r = 400$ kV is given by:

$$\underline{S}_{nat} = \frac{U_r^2}{\underline{Z}_c^*} = \frac{400000^2}{49,644 + j1,695} = 3219{,}2\text{-j}\,109{,}9\ \left[\text{MW} + \text{jMvar}\right]$$

whose magnitude is $\left|\underline{S}_{nat}\right| = 3221\ [MVA]$. This value is about five times the OHL natural power; consequently, the insulated cable has a greater aptitude for transmission of electric energy.

The complex power at current rating is given by (25) i.e.

$$\underline{S}_R = \sqrt{3} \cdot 400000 \cdot 1788 \cdot (0,98 + j0,2) = 1214 + j248\,[MW + jM\,\text{var}]$$

Therefore, since this power is lower than the natural one, the insulated cable is limited by its thermal behavior even if from a power transmission standpoint, it has a very good behavior.

By fixing $\underline{S}_R = 1214 + j248\,[MW + jMvar]$, and by applying the Ossanna's theorem, the students can easily infer that:

$$\begin{cases} \Delta u \cong 0{,}618\% \\ \Delta P = 3,8\,MW \\ \Delta Q \cong -297\,M\,\text{var} \end{cases}$$

Therefore, the steady-state regime is extremely good with a very low voltage drop and low power losses. It is worth noting that the cable line has a beneficial effect on power factor correction: in fact, the sending-end reactive power is only −54 Mvar.

Many other regimes can be solved: it could be didactical to make the students solve an overload of the 10%, i.e $\underline{S}_R = 1335 + j267\,[MW + jMvar]$.

The results are reported below:

$$\begin{cases} \Delta u \cong 0{,}751\% \\ \Delta P = 4,6\,MW \\ \Delta Q \cong -287M\,\text{var} \end{cases}$$

The regime is still extremely good. With regard to the aspects deriving from the line energization, by hypothesizing, as in Sect. A, two limit equivalent impedances $\underline{Z}''_{weak} \cong j21,905$ and $\underline{Z}''_{strong} \cong j4,5276$, (21) gives the two overvoltage limits for the weakest node and for the strongest one, i.e.:

$$\underline{U}''_{oR} = \frac{U_0}{\underline{A} + Z''_{strong} \cdot \underline{C}} = 233730\text{-}j100,34\ V \rightarrow \left|\underline{U}''_{oR}\right| \cong 233,73\,kV$$

$$\underline{U}''_{oR} = \frac{U_0}{\underline{A} + Z''_{weak} \cdot \underline{C}} = 243178\text{-}j114,1\ V \rightarrow \left|\underline{U}''_{oR}\right| \cong 243,18\,kV$$

In case of the insulated cable with d = 30 km, (23) is not verified only for the weakest node energization:

$$\left|\underline{U}''_{oR}\right| \geq 420/\sqrt{3} = 242,5\ \text{kV}$$

In this way, the students should fix in their minds the very important concept of best-end switching [20]. Regarding the no-load switching current, it is:

$$\underline{I}_{NL} = \frac{U_0}{\underline{A}/\underline{C}} = 0,499 + j509,28\,A$$

The magnitude of $\underline{I}_{NL}$ is greater than $I_c = 400$ A and therefore the switching rated current constraint $|\underline{I}_{NL}| \leq I_c = 400$ A is not verified.

An interesting exercise for the students could be to answer the following question: which is the maximum length of the insulated cable in order to fulfil the constraint of rated capacitive switching current?

The solution is $d = 23{,}6$ km (the solution can be found analytically only if the insulated cable were ideal ($r = g = 0$), otherwise the students must find it by attempts).

The professor can increase the length of the insulated cable and add the shunt compensations at both ends or at intermediate points along the cable. The students can again apply the settlement presented in this paper after having obtained the transmission matrix equivalent to the cascade connection of the cable sections and of the shunt reactors as the ordered product of all the transmission matrixes.

C. GAS-INSULATED LINES [17], [21], [22]

The natural power with reference to the voltage $U_r = 400$ kV is given by:

$$\underline{S}_{nat} = \frac{U_r^2}{\underline{Z}_c^*} = \frac{400000^2}{62,849 + \text{j}4} = 2535{,}5\text{-j}161{,}51\ \left[\text{MW} + \text{jMvar}\right]$$

whose magnitude is $\left|\underline{S}_{nat}\right| \cong 2541\,[MVA]$. This value is about four times greater than the OHL natural power, but it is 0,8 times lower than the cable one. Consequently, the gas-insulated line would have an aptitude for transmission of electric energy greater than OHL but lower than insulated cable. The complex power at current rating is given by (25) i.e.

$$\underline{S}_R = \sqrt{3} \cdot 400000 \cdot 2390 \cdot (0,98 + j0,2) = 1623 + j330\,[MW + jM\,\text{var}]$$

Therefore, being this power lower than $\underline{S}_{nat}$, the gas-insulated line is limited by its thermal constrain even if from a power transmission standpoint, it has a good behavior.

By fixing $\underline{S}_R = 1623 + j330\,[MW + jMvar]$, the students must apply the Ossanna's theorem, so to obtain:

$$\begin{cases} \Delta u \cong 2{,}04\% \\ \Delta P = 15,1\,MW \\ \Delta Q \cong -148,7\,M\,\text{var} \end{cases}$$

The steady-state regime is very good with a low voltage drop and low power losses.

For exercise, the students can solve other regimes as those in Table 5. The first row is the no-load regime: the voltage drop Δu has a minus sign, i.e. it is an overvoltage due to the

TABLE 5. Steady-state regimes of the gas-insulated line of table 2 with d = 100 km.

$\underline{S}_R$ [MW+jMvar]	$\frac{Q_R}{P_R}$	$\lvert\underline{U}_{oR}\rvert$ kV	$\lvert\underline{U}_{oS}\rvert$ kV	ϑ °	Δu %	ΔP MW	ΔQ Mvar	Δ_p %	$\lvert\underline{I}_R\rvert$ A	$\lvert\underline{I}_S\rvert$ A	$\frac{\max(I_R, I_S)}{I_{cur\_rat}}$
0,00+j0,00	/	231,33	230	0,042	-0,576	0,135	-272,770	/	0	395,3	0,165
2535,5-j161,51	-0,064	230,94	232,53	6,123	0,688	34,998	-2,24	1,380	3667,1	3692,3	1,545

Ferranti's effect. The second row is the natural power regime by fixing a voltage at sending-end equal to 232,53 kV: from the theory, the voltage drop, power losses and reactive power required by the line should be about:

$$\begin{cases} \Delta u \cong k'd = 0{,}685\% \\ \Delta p \cong 2 \cdot k'd = 1{,}37\% \\ \Delta q \cong 2 \cdot k'd = 1{,}37\% \end{cases}$$

These values are almost completely confirmed. With regard to the aspects deriving from the line energization, by hypothesizing, as in Sect. A, two limit equivalent impedances $\underline{Z}''_{weak} \cong j21,905$ and $\underline{Z}''_{strong} \cong j4,5276$, (21) gives the two overvoltage limits for the weakest node and for the strongest one i.e.:

$$\underline{U}''_{oR} = \frac{U_0}{\underline{A} + Z''_{strong} \cdot \underline{C}} = 233150\text{-}j173,54\ V \rightarrow \left|\underline{U}''_{oR}\right| \cong 233,15\,kV$$

$$\underline{U}''_{oR} = \frac{U_0}{\underline{A} + Z''_{weak} \cdot \underline{C}} = 240,383\text{-}j0,183\ V \rightarrow \left|\underline{U}''_{oR}\right| \cong 240,4\,kV$$

In case of the gas-insulated line with d = 100 km, (23) is always verified i.e.

$$\left|\underline{U}''_{oR}\right| \leq 420/\sqrt{3} = 242,5\ \text{kV}$$

About the no-load switching current, it is:

$$\underline{I}_{NL} = \frac{U_0}{\underline{A}/\underline{C}} = 0,195 + j395,32\,A$$

whose magnitude is slightly lower than $I_c = 400$ A i.e. the inequation $|\underline{I}_{NL}| \leq I_c = 400$ A is verified.

This implies that d = *100* km is approximately the limit length for no-load switching current.

Longer GILs need a suitable shunt compensation.

D. HYBRID TRANSMISSION LINES: CASCADE CONNECTION OF OVERHEAD, CABLE AND GAS-INSULATED LINES [23]–[25]

Hybrid lines are an interesting possibility to overcome geographical limits or oppositions to the erection of an entirely overhead line.

The professor can ideate any combination of cascade connection of the three abovementioned transmission line typologies with or without shunt reactive compensation.

E. THE VOLTAGE COLLAPSE [26]

The last application of the Ossanna's theorem could be the drawing of the classical "nose curve" due to the voltage collapse. In fact, as already mentioned, it can be ascertained that the phasors $\underline{u}_2$, by (16), gives a precise reference for the voltage collapse.

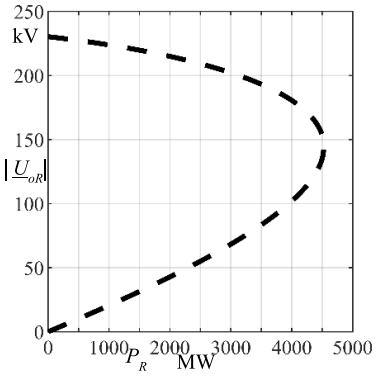

FIGURE 4. Voltage collapse of the overhead line d = 50 km in Table 2.

Therefore, the students can storage the two vectors $\underline{u}_1$ form (15) and $\underline{u}_2$ from (16) by increasing the receiving-end active power.

By plotting as x-axis, the receiving-end active power and as y-axis the receiving-end voltage magnitudes of $\underline{u}_1$ and $\underline{u}_2$, it is possible to obtain the curve of Fig. 4.

Only this use of Ossanna's theorem allows the students to avoid the cumbersome formulae [27] commonly used to obtain the "nose curve".

VI. CONCLUSION

The paper presents the power education approach used in the Department of Industrial Engineering at the University of Padova. The extensive use of Ossanna's theorem, together with other original formulae of no-load switching current and overvoltages due to the line energization, gives the students a powerful tool to understand the impact of steady-state regimes of symmetric electric lines. Moreover, the paper shows how the voltage collapse can also be evaluated in a very simple manner. During the last ten years, this approach has proven to increase the awareness of the students regarding the actual issues of the power systems. Moreover, our graduate students, employed in the Italian Transmission and Distribution System Operators, witness that they continue using these concepts during their working activities.

Furthermore, the authors wish to highlight that, potentially, Ossanna's theorem could be applicable to large power systems for solving *analytically* the power flow by avoiding iterative procedures. Of course, a lot of research (and a stroke of genius) is necessary to verify if this is possible. In this case, it would not be a didactical result but a very important scientific contribution to power system community.

APPENDIX
ITERATIVE PROCEDURES

Let us suppose to solve the regime of row 6 in Tab. 4. A first tentative chosen voltage magnitude can be $\underline{U}_{oR} = 210$ kV so to compute

$$\underline{I}_R = \frac{\underline{S}^*_{oR}}{\underline{U}^*_{oR}} = 3,1746\text{-}j0,635\,kA$$

By means of (1), the value of $\underline{U}_{os}$ can be derived i.e.:

$$\underline{U}_{oS} = \underline{A} \cdot \underline{U}_{oR} + \underline{B} \cdot \underline{I}_R = 221,605 + \text{j}\,42{,}178\,\text{kV}$$

whose magnitude 225,583 kV is different from the fixed voltage 230 kV. Then, a magnitude value greater than 0,1 kV is newly chosen for $\underline{U}_{oR}$ and the same aforementioned procedure iterates. By setting a precision of *0, 1* kV, in *49* iterations, the regime is solved with a solution equal to $U_{oR} = 214{,}9$ kV versus the exact value of $U_{oR} = 214{,}957$ kV by Ossanna's theorem. The iterative method needs to have a first tentative value as close as possible to the right solution otherwise thousands of iterations are needed: therefore, it is cumbersome and much less effective than an analytical solution and, furthermore it does not allow evaluating the phenomenon of the voltage collapse.

ACKNOWLEDGMENT

The paper is dedicated to the memory of Professor Antonio Paolucci who always advocated the importance of Ossanna's theorem in power system analysis. From above, Antonio rejoices over his dream coming true: a School of electric energy transmission at the University of Padova.

REFERENCES

[1] J. Ossanna, "Neue Arbeitsdiagramme über die Spannungsänderung in Wechselstromnetzen," *EuM*, 1926.
[2] J. Ossanna, "Fernübertragungsmöglichkeiten grosser Energiemengen," *ETZ*, 1922.
[3] Y. Hase, *Handbook of Power System Engineering*. Chichester, U.K.: Wiley, 2007.
[4] A. von Meier, *Electric Power Systems: A Conceptual Introduction*. Hoboken, NJ, USA: Wiley, 2006.
[5] J. Schlabbach and K.-H. Rofalski, *Power System Engineering: Planning, Design and Operation of Power Systems and Equipment*. Hoboken, NJ, USA: Wiley, 2014.
[6] F. Saccomanno, *Electric Power Systems: Analysis and Control*. Piscataway, NJ, USA: Institute of Electrical and Electronics Engineers, 2003.
[7] R. Benato and A. Paolucci, *EHV AC Undergrounding Electrical Power: Performance and Planning* (Power Systems), vol. 47. Springer, 2010, doi: 10.1007/978-1-84882-867-4.
[8] C. A. Gross, *Power System Analysis*. Hoboken, NJ, USA: Wiley, 1989.
[9] R. Benato, R. Caldon, A. Chiarelli, M. Coppo, C. Garescì, S. Dambone Sessa, D. Mimo, M. Modesti, L. Mora, and F. Piovesan, "CALAJOULE: An italian research to lessen joule power losses in overhead lines by means of innovative conductors," *Energies*, vol. 12, no. 16, p. 3107, Aug. 2019.
[10] *High Voltage Alternating-Current Circuit-Breakers*, Standard IEC 62271-100, 2001.
[11] R. Benato, S. D. Sessa, and F. Guglielmi, "Determination of steady-state and faulty regimes of overhead lines by means of multiconductor cell analysis (MCA)," *Energies*, vol. 5, no. 8, pp. 2771–2793, Jul. 2012.
[12] R. Benato, S. D. Sessa, F. Guglielmi, E. Partal, and N. Tleis, "Zero sequence behaviour of a double-circuit overhead line," *Electr. Power Syst. Res.*, vol. 116, pp. 419–426, Nov. 2014.
[13] M. Wang, M. Yang, J. Wang, M. Wang, and X. Han, "Contingency analysis considering the transient thermal behavior of overhead transmission lines," *IEEE Trans. Power Syst.*, vol. 33, no. 5, pp. 4982–4993, Sep. 2018.
[14] G. J. Anders, *Rating of Electric Power Cables in Unfavourable Thermal Environment*. Hoboken, NJ, USA: Wiley, 2005.
[15] R. Benato and A. Paolucci, "Operating capability of long AC EHV transmission cables," *Electr. Power Syst. Res.*, vol. 75, no. 1, pp. 17–27, Jul. 2005.
[16] R. Benato, L. Colla, S. D. Sessa, and M. Marelli, "Review of high current rating insulated cable solutions," *Electr. Power Syst. Res.*, vol. 133, pp. 36–41, Apr. 2016.
[17] R. Benato, C. Di Mario, and H. Koch, "High-capability applications of long gas-insulated lines in structures," *IEEE Trans. Power Del.*, vol. 22, no. 1, pp. 619–626, Jan. 2007.
[18] S. Y. King and N. A. Halfter, *Underground Power Cables*. London, U.K.: Longman, 1982.
[19] E. Peschke and E. von Olshausen, *Cable Systems for High and Extra-High Voltage*. Berlin, Germany: Publicis MDC Verlag, 1999.
[20] D. F. Oakeshott, "Control of switching surges," in *Modern Power Station Practice: EHV Transmission*, 3rd ed. Oxford, U.K.: Pergamon Press, 1991, ch. 9, sec. 3.3.
[21] R. Benato, F. Dughiero, M. Forzan, and A. Paolucci, "Proximity effect and magnetic field calculation in GIL and in isolated phase bus ducts," *IEEE Trans. Magn.*, vol. 38, no. 2, pp. 781–784, Mar. 2002.
[22] H. Koch, *Gas-Insulated Transmission Lines (GIL)*. Hoboken, NJ, USA: Wiley, 2012.
[23] R. Benato and A. Paolucci, "Operating capability of AC EHV mixed lines with overhead and cables links," *Electr. Power Syst. Res.*, vol. 78, no. 4, pp. 584–594, Apr. 2008.
[24] F. M. Gatta and S. Lauria, "Very long EHV cables and mixed overhead-cable lines. Steady-state operation," in *Proc. IEEE Russia Power Tech*, St. Petersburg, Russia, Jun. 2005, pp. 1–7
[25] F. Barakou, L. Wu, P. A. A. F. Wouters, and E. F. Steennis, "Investigation of the necessary modeling depth in transmission systems with mixed OHL-cable configuration," in *Proc. 10th Int. Conf. Compat., Power Electron. Power Eng. (CPE-POWERENG)*, Bydgoszcz, Poland, Jun. 2016, pp. 70–75.
[26] L. Zheng, W. Hu, Y. Min, and J. Ma, "A novel method to monitor and predict voltage collapse: The critical transitions approach," *IEEE Trans. Power Syst.*, vol. 33, no. 2, pp. 1184–1194, Mar. 2018.
[27] P. Kundur, *Power System Stability and Control*. New York, NY, USA: McGraw-Hill, 1994.

ROBERTO BENATO (Senior Member, IEEE) was born in Venezia, Italy, in 1970. He received the Dr.Ing. degree in electrical engineering from the University of Padova, in 1995, and the Ph.D. degree in power systems analysis, in 1999. Since 2011, he has been as an Associate Professor with the Department of Industrial Engineering, Padova University. He is the author of 190 articles and four books, edited by Springer, Wolters Kluwer, and China Machine Press. He has been member of seven Cigré Working Groups (WGs) and secretary of two Joint WGs. He has also been a member of the IEEE PES Substations Committee. He has been nominated Member of the IEC TC 120 Electrical Energy Storage (EES) Systems, in 2014. He is currently a Corresponding Member of Cigré WG B1.72 Cable rating verification 2nd part. He is also a member of Italian AEIT. He has been elevated to the grade of CIGRÉ Distinguished Member, in 2018.

SEBASTIAN DAMBONE SESSA (Member, IEEE) was born in Venezia, Italy, in 1981. He received the Dr.Ing. degree in electrical engineering from the University of Padova, in 2010, and the Ph.D. degree in power systems analysis, in 2017. He was appointed as a Research Associate with the Department of Industrial Engineering, Padova University, in 2017. His main research interests include transmission line modeling, fault location algorithms, stationary electrochemical and hybrid energy storage, and high-voltage direct current installations. He has been member of the Cigré working groups B1.47, B1.45, and B1.56. He is a member of Italian AEIT.